

## Macroscopic description of quantum-mechanical tunneling

M. G. Ancona

*Naval Research Laboratory (Code 6813), Washington, D.C. 20375-5000*

(Received 7 November 1989; revised manuscript received 27 February 1990)

Recently a macroscopic description of electron transport in semiconductors was developed [M. G. Ancona and H. F. Tiersten, *Phys. Rev. B* **35**, 7959 (1987)] that incorporates lowest-order quantum effects by endowing the electron gas with a density-gradient-dependent equation of state. Calculations made using this new description have been found to agree well with corresponding results obtained with use of one-electron quantum mechanics for various equilibrium (no current flow) situations. In the present paper, the density-gradient theory is applied to a quantum transport problem. The equations of nonequilibrium density-gradient theory are discussed first in general terms and then as applied to the specific example of steady-state tunneling through a metal-insulator-metal barrier with thermionic and space-charge effects (to be examined in a future paper) neglected. Two different tunneling regimes, which may be described as inertia dominated and bulk-scattering dominated, are analyzed, and approximate expressions for the current-voltage characteristics in each regime are given. For inertia-dominated tunneling, we devise "virtual-anode" boundary conditions to account for dissipation in the downstream contact and obtain results which compare favorably with those of standard elastic-tunneling theory.

### I. INTRODUCTION

A macroscopic (or continuum or hydrodynamic) theory of electron transport in semiconductors has long been of great practical value in the form of the diffusion-drift (DD) description of Van Roosbroeck.<sup>1</sup> However, in recent years, with reductions in the temporal and spatial scales germane to state of the art and possible future semiconductor devices, various deficiencies in this description have become apparent. Awareness of these flaws combined with the need for modeling tools useful in the new regimes, has led researchers (i) to devise corrections to diffusion-drift theory such as "energy transport" theory<sup>2</sup> or Thornber's equation<sup>3</sup> and (ii) to pursue microscopic transport theory, e.g., solving Boltzmann<sup>4</sup> or Liouville<sup>5</sup> equations. Of these approaches, the former has been regarded as completely classical; for describing quantum effects it is widely believed that a microscopic theory is required. This belief is often incorrect. In a recent paper,<sup>6</sup> we showed that the inability of the diffusion-drift theory to describe quantum effects can be partially rectified by making the equation of state of the electron gas *density-gradient* dependent. With this generalization, the diffusion-drift theory was often found to accurately describe quantum-confinement effects in static (no current flow) semiconductor situations.<sup>6-8</sup> Subsequently, a direct connection to quantum-statistical mechanics was established.<sup>9</sup> In the present paper, we continue this development by exhibiting the use of the density-gradient theory in situations in which currents flow; in particular, steady-state tunneling in metal-insulator-metal (MIM) structures is examined.<sup>10</sup>

The macroscopic approach to electron transport theory employed here includes the lowest-order effects of quantum mechanics on transport in a mathematically consistent and physically correct manner.<sup>6,9</sup> The neglect

of higher-order quantum effects, e.g., various interference phenomena,<sup>8,11</sup> makes the theory much simpler than alternative microscopic quantum transport theories. Because of this and because the macroscopic theory is formulated in more familiar and physically intuitive "classical" language, when it is applicable, it should provide an efficient tool for studying semiconductor device situations in which quantum transport phenomena are significant. In particular, it allows other physical complications associated with real devices such as geometry, scattering (inelastic tunneling), electrostatics, and boundary effects to be included and analyzed more readily. In addition, as an extension of a well-studied theory, the macroscopic approach to quantum transport theory can directly benefit from the existing wealth of numerical techniques and simulation experience in both diffusion-drift modeling and fluid dynamics.

Although the density-gradient theory is formulated in "classical" terms, it should be recognized that like any continuum theory it stands independent of the dichotomy between classical and quantum mechanics. Thus, in relation to transport across a "barrier," the fact that a potential barrier is a classically forbidden region has no bearing on the applicability of the continuum analysis. We simply no longer view the barrier as an ideal insulator; it is merely a solid—a generalized semiconductor—through which (quantum) conduction occurs. While it is impossible to localize individual charges inside the barrier there is nonetheless charge *density* inside the barrier and it is this that the continuum theory is concerned with. Of course, in order for the theory to apply, the tunneling situation must permit continuum assumptions<sup>12</sup> and as a result there are tunneling problems which are outside its scope, e.g., an analysis of a quantum "dot."

Finally, it is important to distinguish our work from other hydrodynamic treatments of quantum mechanics.

The most well known of these is that of Madelung,<sup>13</sup> de Broglie<sup>14</sup> and Bohm.<sup>15</sup> In contrast to the density-gradient theory, Madelung's theory is not a macroscopic (continuum) description. It is microscopic, including both the amplitude *and* the phase aspects of quantum mechanics and is, in fact, precisely equivalent to quantum mechanics.<sup>15</sup> As discussed in Ref. 8, a partial equivalence between Madelung's theory and the density-gradient theory exists only in a low-density, low-temperature limit when all electrons are in the lowest-(pure) energy state or subband. A second hydrodynamic formulation of quantum mechanics which has recently appeared<sup>16</sup> also deserves mention. This work has much more in common with our approach and is based on an application of Grad's expansion<sup>17</sup> of classical kinetic theory to Wigner's formulation of quantum-statistical mechanics. The relation between Ref. 16 and our work is much the same as that, in a classical context, between Grad's analysis<sup>17</sup> and the earlier work of Burnett.<sup>18</sup>

This paper is organized as follows. In Sec. II we provide a brief introduction to the density-gradient theory in the particular chemical-potential form in which it is used in this work. The remainder of the paper then applies this theory to one-dimensional, steady-state MIM tunneling. The general MIM boundary value problem is formulated in Sec. III. This is then solved both in an approximate analytical fashion and numerically in the succeeding two sections for two limiting cases: inertia-dominated tunneling (Sec. IV) and drag or bulk-scattering-dominated tunneling (Sec. V). The former corresponds to elastic tunneling in the conventional microscopic approach,<sup>5,19</sup> while the latter has not previously been analyzed. For inertia-dominated tunneling, energy is dissipated (and entropy produced) only at the contacts and, to properly account for this, we develop approximate "virtual-anode" boundary conditions (Sec. IV). The paper ends with a short summary (Sec. VI).

## II. DENSITY-GRADIENT THEORY: CHEMICAL-POTENTIAL FORMULATION

Lowest-order quantum effects can be included in a macroscopic description of electron transport in a semiconductor by requiring that the internal energy of the electron gas depend not only on electron density but also on the density gradient.<sup>6-9</sup> With this generalization, the transport theory, which may be called *density-gradient theory*, is essentially the hydrodynamics of a density-gradient-dependent solid-state plasma. In its most fundamental form, density-gradient theory is written in terms of the electron-gas pressure. However, by recasting the theory in terms of a chemical potential, a particularly useful derivative theory—which we term *generalized diffusion-drift (GDD) theory* since it reduces to the standard DD theory when the density-gradient effects are neglected—is obtained.<sup>6</sup> GDD theory is precisely equivalent to the pressure formulation except when inertia is important. For cases when inertia is nonnegligible, e.g., many tunneling problems (see below), we have ex-

tended the chemical-potential formulation in an approximate fashion which should be valid under most circumstances and is, in fact, exact for one-dimensional (1D) problems.<sup>6</sup> In this paper, the GDD form of density-gradient theory is used to analyze a 1D quantum transport situation.

In standard DD theory the electron gas is modeled as an ideal gas, i.e., the electron-gas pressure is proportional to the electron charge density  $\rho$  ( $\equiv -qn$ ). The internal energy of the gas (per charge),  $\epsilon$ , depends solely on  $\rho$  and the chemical potential defined by

$$\varphi^e \equiv \frac{\partial(\rho\epsilon)}{\partial\rho}, \quad (2.1a)$$

is that of a Maxwell gas

$$\varphi^e(\rho) = \varphi_B^e - \frac{kT}{q} \ln(\rho/\rho_B), \quad (2.1b)$$

where  $\varphi_B^e$  and  $\rho_B$  are constants. To generalize DD theory to density-gradient theory, we make  $\epsilon$  dependent not only on  $\rho$  but also on the density gradient  $\nabla\rho$ . In this case,  $\varphi^e$  of (2.1a) is replaced by a generalized chemical potential,<sup>6</sup>

$$\varphi^{e*}(\rho, \nabla\rho) = \frac{\partial(\rho\epsilon)}{\partial\rho} - \nabla \cdot \left[ \rho \frac{\partial\epsilon}{\partial\nabla\rho} \right]. \quad (2.2)$$

At lowest order the equation for  $\epsilon$  is<sup>6</sup>

$$\epsilon(\rho, \nabla\rho) = \epsilon_0(\rho) - \frac{b}{2} \left[ \frac{\nabla\rho}{\rho} \right]^2, \quad (2.3)$$

where the proportionality constant  $b$  (which may be weakly density dependent<sup>7</sup>) is a new macroscopic coefficient measuring the strength of the gradient dependence in the electron gas. From the point of view of the classical field theory,  $b$  is to be determined either by an appropriate experiment or by microscopic calculation. That this gradient dependence expresses the lowest-order (macroscopic) effects of quantum mechanics on the electron gas [apart from effects associated with quantum statistics which alter  $\epsilon_0(\rho)$ ] has been demonstrated by the equilibrium calculations of Refs. 6–8, by the steady-state tunneling results of this paper and by the quantum-mechanical derivation given in Ref. 10. In the latter work an explicit connection between the macroscopic theory and mixed-state quantum mechanics was established in the high-temperature limit. In this limit the microscopic formula for  $b$  is  $b = \hbar^2/(12m^*q)$ , where  $m^*$  is the electron effective mass. In the opposite limit of low temperatures and low densities,<sup>8</sup>  $b$  tends toward  $\hbar^2/(4m^*q)$  and, in this case (assuming no scattering), the theory is equivalent<sup>8</sup> to the amplitude part of the Madelung, de Broglie, and Bohm hydrodynamic formulation of (one-electron) quantum mechanics.<sup>13-15</sup>

The equation expressing momentum balance in the electron gas, when written in chemical-potential form, is<sup>6</sup>

$$\nabla(\varphi + \varphi^{e*}) - \mathbf{E}^e = \alpha \frac{d\mathbf{v}}{dt}, \quad (2.4a)$$

where  $\varphi$  is electric potential,  $\mathbf{E}^e$  is the drag force (per

charge) felt by the electrons as they flow through the lattice,  $\mathbf{v}$  is the velocity of the gas,  $\alpha$  is the effective mass to charge ratio of the electrons and

$$\frac{d}{dt} \equiv \frac{\partial}{\partial t} + \mathbf{v} \cdot \nabla. \quad (2.4b)$$

In order to use (2.4a), in addition to the expression for  $\varphi^{e*}$  in (2.2), we need a constitutive relation for  $\mathbf{E}^e$ . The simplest form is the linear drag assumption made by DD theory,<sup>20</sup>

$$\mathbf{E}^e = \mathbf{v} / \mu, \quad (2.5)$$

where  $\mu$  is the mobility of the electron gas. As a first-order approach to introducing scattering (of all types except electron-electron) into a description of tunneling, (2.5) may be reasonable.<sup>21</sup> Of course, for many tunneling problems bulk scattering is negligible and  $\mu \rightarrow \infty$ .

Assuming  $\epsilon_0$  in (2.3a) to be that for a Maxwell gas, from (2.2) and (2.3) we have

$$\varphi^{e*}(\rho, \nabla\rho) = \varphi_B^e - \frac{kT}{q} \ln(\rho/\rho_B) + 2b \frac{\nabla^2 s}{s}, \quad (2.6)$$

where  $s \equiv \sqrt{-\rho}$ . And, inserting this together with (2.5) into (2.4), we obtain the generalized diffusion-drift current equation for the density-gradient-dependent electron gas:

$$\mathbf{J} = \mu\rho \nabla\varphi - D\nabla\rho + 2b\mu\rho \nabla \left[ \frac{\nabla^2 s}{s} \right] - \alpha\mu\rho \frac{d\mathbf{v}}{dt}. \quad (2.7)$$

When both the density-gradient and inertial effects are neglected from (2.7), as expected, the standard DD current equation is recovered. The important term in (2.7) is the density-gradient term,  $2b\mu\rho \nabla(\nabla^2 s/s)$ , which represents an additional current component arising from effects of quantum mechanics manifested on a macroscopic scale. Because this quantum current flows as a result of a gradient in the generalized chemical potential  $\varphi^{e*}$ , it may be referred to as a “quantum-diffusion” current. In situations involving quantum wells, a balance between this current and the usual drift current describes quantum confinement effects<sup>6-8</sup> while, as seen below, in circumstances with transport through barriers, the quantum diffusion current is a tunneling current.

The complete field theory capable of analyzing many quantum transport situations consists of (2.7) plus equations of electrostatics (or electrodynamics), charge balance and thermodynamics plus various constitutive equations, and a consistent set of boundary conditions. Most of these equations appear in Ref. 6 and are introduced below only as needed. For this paper we shall further specialize the theory to steady-state, in which case (2.7) may be written as

$$\frac{\mathbf{J}}{\mu\rho} = \nabla \left[ \varphi + \varphi_B^e - \frac{kT}{q} \ln(\rho/\rho_B) + 2b \left[ \frac{\nabla^2 s}{s} \right] - \frac{\alpha}{2} \mathbf{v} \cdot \mathbf{v} \right] \equiv \nabla\Psi, \quad (2.8)$$

where  $\Psi$ , the “kinetic electrochemical potential,” is the

sum of the electric potential, chemical potential, and kinetic energy per charge.

### III. BOUNDARY-VALUE PROBLEM FOR MIM TUNNELING IN STEADY STATE

In the standard treatment of tunneling through a barrier,<sup>19,22</sup> the electrons are described microscopically using one-electron, effective-mass quantum mechanics, while the barrier is treated macroscopically as an averaged potential-energy variation (often including an assumed solution to a coupled macroscopic electrostatics problem known as the “image force”). In contrast, in the continuum theory approach, both the barrier and the electrons are treated macroscopically and all microscopic details are averaged out at the start. What remains is a boundary-value problem composed of a set of coupled partial differential equations (including the electrostatics) and boundary conditions in macroscopic variables such as electron charge density, electron fluid velocity, chemical potential, etc.

A boundary-value problem of this type is readily formulated within the density-gradient theory outlined in Sec. II. However, such a formulation would fail to account for one important aspect of many tunneling situations and, consequently, a further extension of the theory is required. The complication is not a quantum-mechanical effect *per se* but rather a feature of any transport which is dissipationless over some macroscopic distance. Thus, the same extension would apply to a diffusion-drift description of ballistic transport. Dissipationless electron transport (via elastic tunneling or ballistic transport) implies that the kinetic electrochemical potential  $\Psi$  of the electron gas will remain constant as the gas flows from some initial “starting point” at which  $\Psi$  is known. This is seen directly from (2.8) with  $\mu \rightarrow \infty$ . In the MIM structure under bias, the two metal contacts have different known  $\Psi$ 's and therefore, under conditions of elastic tunneling (and assuming  $\Psi$  is continuous across the contact interfaces), the  $\Psi$  of the electron gas inside the barrier will depend on which side of the barrier the gas originated on. We are thus led to define two distinct electron subpopulations inside the barrier, corresponding to the two electrical contacts from which they issue, each of which is governed by its own transport equation (2.8). Of course, when significant numbers of lattice collisions occur, transport with dissipation is obtained ( $\mathbf{E}^e \neq 0$ ) and the two-fluid model can be reduced to a single electron-gas picture. It is unclear to us whether tunneling is ever observed in this one-fluid bulk-scattering-dominated limit and we therefore pursue the more general two-fluid description. Nevertheless, in Sec. V we present a brief discussion of the characteristics to be expected for bulk-scattering-dominated tunneling.

We consider here a MIM barrier in which only electron conduction (tunneling) is important, i.e., hole tunneling is neglected. As noted earlier, inside the insulator this conduction is divided into two components (subscripts 1 and 2) and we assume one-dimensional, steady-state conditions apply. Employing the coordinate system shown in Fig. 1, from (2.8) the transport equations are

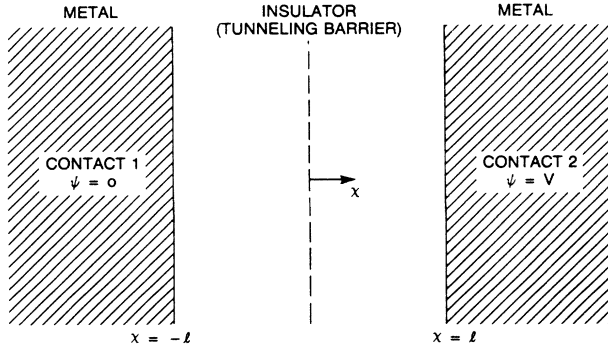


FIG. 1. Schematic of the MIM tunneling structure.

$$J_1 = -\mu s_1^2 \left[ \varphi + \varphi_B^e - 2 \frac{kT}{q} \ln(s_1/s_{1B}) + 2b \frac{s_1''}{s_1} - \frac{\alpha}{2} v_1^2 \right]', \quad |x| \leq l \quad (3.1a)$$

$$J_2 = -\mu s_2^2 \left[ \varphi + \varphi_B^e - 2 \frac{kT}{q} \ln(s_2/s_{2B}) + 2b \frac{s_2''}{s_2} - \frac{\alpha}{2} v_2^2 \right]', \quad |x| \leq l \quad (3.1b)$$

where  $()'$  denotes  $d()/dx$ . We assume trapping in the insulator is negligible and so, from charge conservation,  $J_1$  and  $J_2$  are constants. The differential system is completed by the equation of electrostatics,

$$\varphi'' = \frac{1}{\epsilon_i} (s_1^2 + s_2^2), \quad |x| \leq l \quad (3.1c)$$

where  $\epsilon_i$  is the permittivity of the insulator.

The boundary conditions to be applied to generalized diffusion-drift boundary-value problems were presented in Ref. 6. As applied to the MIM tunneling problem, these consist of the usual electrostatic conditions,

$$\varphi = 0 \text{ at } x = -l \text{ and } \varphi = V \text{ at } x = l, \quad (3.2a)$$

where  $V$  is the voltage (assumed positive) applied across the barrier plus various conditions on the two electron gases. The latter may be divided into "upstream" conditions

$$\left[ \varphi_1^{e*} - \frac{\alpha}{2} v_1^2 \right]_{x=-l} = 0 \quad \text{and} \quad \left[ \varphi_2^{e*} - \frac{\alpha}{2} v_2^2 \right]_{x=l} = 0, \quad (3.2b)$$

$$s_1 = s_M \text{ at } x = -l \text{ and } s_2 = s_M \text{ at } x = l, \quad (3.2c)$$

and "downstream" conditions

$$\left[ \varphi_1^{e*} - \frac{\alpha}{2} v_1^2 \right]_{x=l} = f_1 \quad \text{and} \quad \left[ \varphi_2^{e*} - \frac{\alpha}{2} v_2^2 \right]_{x=-l} = f_2, \quad (3.2d)$$

$$s_1 = s_{1M} \text{ at } x = l \text{ and } s_2 = s_{2M} \text{ at } x = -l, \quad (3.2e)$$

where  $[A]$  signifies the discontinuity in  $A$  across the interface. The terms "upstream" and "downstream," that the right-hand sides of Eqs. (3.2b) are zero and that the right-hand sides of Eqs. (3.2c) equal  $s_M$  (where  $s_M^2$  is the known electron charge density in the contacts which is assumed to be the same at each end) reflect the associations of fluid 1 with the contact at  $x = -l$  and fluid 2 with the contact at  $x = l$ . The quantities  $f_1$  and  $f_2$  in (3.2d) are the forces (per charge) exerted by the interfaces on the two conducting gases<sup>20</sup> and  $s_{1M}^2$  and  $s_{2M}^2$  are the electron densities in the downstream contacts which depend on the rates of "recombination" in the contacts, i.e., the rate at which fluid 1 is "converted" or "thermalized" into fluid 2 at  $x = l$  or vice versa at  $x = -l$ .

There are several other boundary conditions in addition to (3.2) which must, in general, be satisfied at semiconductor interfaces<sup>6</sup> but either are not independent of (3.2) or are identically satisfied in the steady-state MIM conduction problem. Among these are the conditions of charge conservation which can be shown to lead to

$$\frac{\partial \sigma_1}{\partial t} = J_1 + \Gamma_1 \text{ at } x = l \quad \text{and} \quad \frac{\partial \sigma_2}{\partial t} = J_2 - \Gamma_2 \text{ at } x = -l, \quad (3.3)$$

where  $\sigma_1$  and  $\sigma_2$  are surface charge densities and  $\Gamma_1$  and  $\Gamma_2$  are the "recombination" (thermalization) rates of the two tunneling gases into single conducting gases in each of the downstream contacts as a result of scattering. We assume the contacts are such that this occurs entirely at the boundary. For a general non-steady-state boundary-value problem (3.3) is independent of (3.2) and would be used (along with the electrostatic condition  $\sigma = \sigma_1 + \sigma_2 = \epsilon_i E$ ), following solution of (3.1) with (3.2), to determine  $\sigma_1$  and  $\sigma_2$  at  $|x| = l$ . In steady state, the surface charge is fixed (only  $\sigma$  can be determined) and these conditions become superfluous: They must contain identical information to the downstream conditions (3.2d). A second set of boundary conditions in density-gradient theory stems from the requirement that at general semiconductor interfaces  $b \partial \rho / \partial n$  must be continuous,<sup>6</sup> however, this condition does not apply here because density-gradient effects are not considered in the contacts.

The above two-point boundary value problem is now well posed. The ten independent boundary conditions (3.2) are precisely the number required to find the eight integration constants of the ordinary differential system (3.1) plus the two currents  $J_1$  and  $J_2$ . In solving this problem the functions  $f_1$  and  $f_2$  in (3.2d) and  $s_{1M}$  and  $s_{2M}$  in (3.2e) must be known. These functions are mathematical models for the thermalization processes occurring in the downstream contacts. In this paper, instead of specifying these functions, we develop some simpler approximate conditions to be used in place of (3.2d) and (3.2e). To this end, we note that the above boundary-value problem avoids any consideration of transport and electrostatics *inside the contacts* by choice of boundary conditions. For example, use of condition (3.2a)—an assumption that the contacts are electrostatically ideal conductors—means that (3.1c) need not be solved inside the contacts. Similarly, (3.2b) and (3.2c)

(with  $s_M$  and  $\varphi_M^{e*}$  known), which may be regarded as defining the *upstream* contacts as ideal with respect to transport, obviate the need to consider the transport in the upstream contact. For the *downstream* contacts, we shall define an ideal contact as having an infinite thermalization rate. In this case,  $s_1$  ( $s_2$ ) will obviously be zero *inside* the downstream contact. However, since  $s_1$  ( $s_2$ ) cannot also be zero inside the barrier (this would imply infinite velocity),  $s_1$  ( $s_2$ ) must suffer a discontinuity at  $x=l$  (at  $x=-l$ ). Thus, in this limit, the continuity conditions (3.2e) are inappropriate and must be dropped. In their place, we assume

$$s'_1 \cong 0 \text{ at } x=l \text{ and } s'_2 \cong 0 \text{ at } x=-l, \quad (3.4a)$$

which may be interpreted as statements that, when the thermalization rate in the contact is infinite, no “back tunneling” (of  $s_1$  at  $x=l$  or  $s_2$  at  $x=-l$ ) occurs and no downstream “quantum” boundary layer forms. The second pair of downstream conditions is given by either (3.2d) or (3.3) which, as noted earlier, contain identical information in steady state. Employing (3.3), we take  $\Gamma_1$  ( $\Gamma_2$ ) proportional to  $\rho_1$  ( $\rho_2$ ) so that these conditions are “surface recombination conditions,”

$$J_1 = -\gamma_1 s_1^2 \text{ at } x=l \text{ and } J_2 = \gamma_2 s_2^2 \text{ at } x=-l, \quad (3.4b)$$

and we assume that the “surface recombination velocities”<sup>23</sup> satisfy  $\gamma_1 = \gamma_2 \equiv \gamma$ . We remark that, since the intrinsic “recombination” rate *in the contacts* is here taken to be infinite, the actual recombination rate and thus  $\gamma$  is determined entirely by inertia and bulk scattering (if this is important). In the case when scattering ( $\mu$ ) is negligible, energy is dissipated only at the contacts and the rate at which this occurs is set by the recombination velocity  $\gamma$ , e.g., at  $x=l$  the energy dissipated per unit area is  $\gamma s_1^2 \varphi_{MB}^e$ , where  $\varphi_{MB}^e \equiv \varphi_M^{e*} - \varphi_B^e$ .

Finally, in the general case when the thermalization rate in the downstream contact is *not* infinite,  $s_1$  ( $s_2$ ) will be nonzero inside the contact, “backtunneling” will occur and  $s'_1$  ( $s'_2$ ) will be less (greater) than zero at the interface. In this case, a “quantum” boundary layer will exist just inside the downstream contact and  $s_1$  ( $s_2$ ) will pass through a minimum at some  $x_{\min} < l$  ( $x_{\min} > -l$ ). We shall refer to the location  $x_{\min}$  as the “*virtual anode*” (in analogy with the concept of a “*virtual cathode*” in emission theory) since it can serve as a convenient point for imposing alternative “boundary” conditions. By definition (3.4a) applies there and we assume (3.4b) does as well with  $\gamma$  now containing contributions not only from inertia but also from the rate of “back tunneling” and from the finite recombination rate in the contact. Lastly, since the recombination rate is likely such that  $s_{1M} \ll s_M$  ( $s_{2M} \ll s_M$ ), the downstream quantum boundary layer will be of negligible thickness and hence we assume  $x_{\min} \cong l$  ( $x_{\min} \cong -l$ ).

#### IV. STEADY-STATE MIM TUNNELING: INERTIA-DOMINATED CASE

In this section we solve the boundary-value problem posed in Sec. III under the further assumptions that drag,

the coupling of the electron density into the electrostatics (space-charge effect), and normal diffusion can be neglected. Negligible drag ( $\mu \rightarrow \infty$ ) corresponds to the case of elastic tunneling, a condition usually assumed in microscopic treatments<sup>22</sup> and frequently met in real tunneling situations. The neglect of space-charge effects depends on the density being low enough, while normal diffusion is negligible at “low” temperatures. As pointed out earlier, the boundary conditions of Sec. III neglect effects of normal diffusion in the contacts as well and, as a result, thermionic emission processes are not modeled. (The interesting case of thermionic field emission will be examined in a future publication.) The net effect of all of these assumptions is that we study conduction through MIM barriers dominated by quantum diffusion (tunneling), by drift in the electric field and by inertial forces. This is of interest because it is mathematically tractable, because it demonstrates that the density-gradient theory can describe many of the well-known characteristics of tunneling and because it shows close correspondence to the usual quantum-mechanical calculation.

The analysis proceeds as follows. Neglecting the effect of space charge, (3.1c) with (3.2a) integrates to

$$\varphi(x) = -E_0(x+l) \text{ where } E_0 \equiv -V/2l, \quad |x| < l. \quad (4.1)$$

With drag negligible, (3.1a) and (3.1b) can be integrated once directly also. Then, by inserting (4.1) into the results, neglecting normal diffusion and employing (3.2b), we obtain

$$-\frac{\alpha J_1^2}{2s_1^4} - E_0(x+l) - \varphi_{MB}^e + 2b \frac{s_1''}{s_1} = 0, \quad |x| \leq l \quad (4.2a)$$

$$-\frac{\alpha J_2^2}{2s_2^4} - E_0(x-l) - \varphi_{MB}^e + 2b \frac{s_2''}{s_2} = 0, \quad |x| \leq l. \quad (4.2b)$$

The boundary value problem consisting of (4.2) with (3.2c) and (3.4) does not have an analytical solution. Below, we obtain some approximate solutions valid in restricted bias regimes. These are then compared both with the full numerical solution and with known microscopic results.

##### A. Regime with $V < \varphi_{MB}^e$ (normal tunneling)

As is evident from (4.2), if  $s_1$  and  $s_2$  are sufficiently large, the inertia terms in (4.2) ( $\alpha J_1^2/2s_1^4$  and  $\alpha J_2^2/2s_2^4$ ) will be negligible. In this case, quantum diffusion and electrostatic drift balance and Eqs. (4.2) becomes

$$2b \frac{s_1''}{s_1} \cong E_0(x-x_1), \quad (4.3a)$$

$$2b \frac{s_2''}{s_2} \cong E_0(x-x_2), \quad (4.3b)$$

where  $x_1 \equiv l(2\varphi_{MB}^e/V - 1)$  and  $x_2 \equiv l(2\varphi_{MB}^e/V + 1)$ . Clearly, a necessary condition for the validity of (4.3) is that their right sides be positive since, if either (4.3a) or (4.3b) passes through a turning point,  $s_1$  or  $s_2$  will vanish somewhere and the corresponding inertia term in (4.2) could not be neglected. From the definitions of  $x_1$  and

$x_2$ , this suggests that (4.3) will be valid throughout the barrier when  $|V| < \varphi_{MB}^e$ . This is the usual requirement for normal (or direct) tunneling in the conventional microscopic approach<sup>22</sup> and, as we shall see, a treatment of inertia-dominated tunneling using (4.3) is, in fact, a description of normal elastic tunneling.

Now, inertia is not generally negligible *throughout* the barrier because  $s_{1M}$  and  $s_{2M}$  in (3.2e), and hence, the densities near the downstream contacts, are typically very small. As a result, Eqs. (4.3) are usually invalid in these regions. However, because these regions are very narrow, it is reasonable to employ (4.3) throughout the barrier and simply absorb the effects of inertia into the virtual-anode boundary conditions. One obvious method for doing this is to assume that inertia just modifies the value of  $\gamma$  in (3.4b) to a new effective value  $\bar{\gamma}$ , i.e.,

$$J_1 = -\bar{\gamma}s_1^2 \text{ at } x=l \text{ and } J_2 = \bar{\gamma}s_2^2 \text{ at } x=-l. \quad (4.4)$$

Alternatively, we could assume  $s_{1M}=s_{2M}=0$  in (3.2e) (without inertia these conditions no longer force infinite velocity) and, in place of (3.4a), we have

$$s_1=0 \text{ at } x=l \text{ and } s_2=0 \text{ at } x=-l. \quad (4.5a)$$

Conditions (4.5a) with (3.4b) imply zero current unless higher-order corrections to (3.5b), i.e., density-gradient terms, are considered. Accordingly, we assume  $\gamma_1 = \gamma_c + \gamma_g(s_1'/s_1)^2$  and  $\gamma_2 = \gamma_c + \gamma_g(s_2'/s_2)^2$  as in (2.3a) and, from (3.4b) with (4.5a), obtain the nontrivial conditions

$$J_1 = -\gamma_g s_1'^2 \text{ at } x=l \text{ and } J_2 = \gamma_g s_2'^2 \text{ at } x=-l. \quad (4.5b)$$

For simplicity in discussion we shall refer to the original virtual anode conditions (3.4) as "VA," the modified conditions (3.4a) and (4.4) as "VM1," and the alternative modified conditions (4.5) as "VM2."

A tunneling analysis based on (4.3), (3.2c), and either VM1 or VM2 is quasistatic since the solutions for  $s_1$  and  $s_2$  are independent of the current [ $J_1$  and  $J_2$  enter only through (4.4) or (4.5b)]. In the inertia-dominated regime (with  $V < \varphi_{MB}^e$ ), this analysis begins by noting that Eqs. (4.3) are Airy equations with general solutions

$$s_1 = C_+ \text{Ai}(r_1) + D_+ \text{Bi}(r_1), \quad |x| \leq l \quad (4.6a)$$

$$s_2 = C_- \text{Ai}(r_2) + D_- \text{Bi}(r_2), \quad |x| \leq l \quad (4.6b)$$

where

$$r_1 \equiv \sqrt[3]{V/4bl} (x_1 - x) \text{ and } r_2 \equiv \sqrt[3]{V/4bl} (x_2 - x).$$

When conditions VM1 are used, from (3.2c) and (3.4a) we determine the constants  $C_\pm$  and  $D_\pm$  to be

$$C_\pm = \frac{-s_M \text{Bi}'(r_\pm)}{\text{Bi}(r_0) \text{Ai}'(r_\pm) - \text{Bi}'(r_\pm) \text{Ai}(r_0)} \quad (\text{VM1}), \quad (4.7a)$$

$$D_\pm = \frac{s_M \text{Ai}'(r_\pm)}{\text{Bi}(r_0) \text{Ai}'(r_\pm) - \text{Bi}'(r_\pm) \text{Ai}(r_0)} \quad (\text{VM1}), \quad (4.7b)$$

where  $r_0 \equiv r_1(x=-l) = r_2(x=l)$  and  $r_\pm \equiv r_1(x=\pm l)$ . Inserting these into (4.6) and noting that, for  $0 < V < \varphi_{MB}^e$ , the turning points of (4.3a) and (4.3b) lie outside the barrier ( $x_1 > l$  and  $x_2 < -l$ ) so that WKB approximations to the Airy functions are appropriate, we obtain the solutions

$$s_1(x) \cong s_M \left( \frac{r_0}{r_1} \right)^{1/4} \frac{\cosh[\frac{2}{3}(r_1^{3/2} - r_+^{3/2})]}{\cosh[\frac{2}{3}(r_0^{3/2} - r_+^{3/2})]}, \quad |x| < l \quad (\text{VM1}), \quad (4.8a)$$

$$s_2(x) \cong s_M \left( \frac{r_0}{r_2} \right)^{1/4} \frac{\cosh[\frac{2}{3}(r_2^{3/2} - r_-^{3/2})]}{\cosh[\frac{2}{3}(r_0^{3/2} - r_-^{3/2})]}, \quad |x| < l \quad (\text{VM1}). \quad (4.8b)$$

And then employing (4.4), the currents are

$$J_1 = -\bar{\gamma}s_1^2(x=l) \cong -\bar{\gamma}s_M^2 \left( \frac{r_0}{r_+} \right)^{1/2} \text{sech}^2[\frac{2}{3}(r_0^{3/2} - r_+^{3/2})] \quad (\text{VM1}), \quad (4.9a)$$

$$J_2 = \bar{\gamma}s_2^2(x=-l) \cong \bar{\gamma}s_M^2 \left( \frac{r_0}{r_-} \right)^{1/2} \text{sech}^2[\frac{2}{3}(r_0^{3/2} - r_-^{3/2})] \quad (\text{VM1}). \quad (4.9b)$$

Finally, the further approximations

$$[\varphi_{MB}^e(\varphi_{MB}^e \pm V)]^{1/2} \cong \varphi^e \pm \frac{V}{2}$$

and

$$\cosh[\frac{2}{3}(r_0^{3/2} - r_\pm^{3/2})] \cong \frac{1}{2} \exp \left[ \frac{2l}{3\sqrt{2b}} \left( \varphi_{MB}^e \pm \frac{V}{2} \right)^{1/2} \right]$$

can be introduced to facilitate comparison with expressions for the tunneling current derived by Simmons<sup>22</sup> and we obtain

$$J = J_1 + J_2 = -4\bar{\gamma}s_M^2 \left\{ \left[ 1 - \frac{V}{\varphi_{MB}^e} \right]^{-1/2} \exp \left[ \frac{-4l}{\sqrt{2b}} \left[ \varphi_{MB}^e - \frac{V}{2} \right]^{1/2} \right] - \left[ 1 + \frac{V}{\varphi_{MB}^e} \right]^{-1/2} \exp \left[ \frac{-4l}{\sqrt{2b}} \left[ \varphi_{MB}^e + \frac{V}{2} \right]^{1/2} \right] \right\} \quad (\text{VM1}). \quad (4.10)$$

In a similar way, for the analysis based on conditions VM2, we find the expressions for the densities and currents to be

$$s_1 \cong s_M \left( \frac{r_0}{r_1} \right)^{1/4} \frac{\sinh[\frac{2}{3}(r_1^{3/2} - r_+^{3/2})]}{\sinh[\frac{2}{3}(r_0^{3/2} - r_+^{3/2})]}, \quad |x| < l \quad (\text{VM2}), \quad (4.11a)$$

$$s_2 \cong s_M \left( \frac{r_0}{r_2} \right)^{1/4} \frac{\sinh[\frac{2}{3}(r_2^{3/2} - r_-^{3/2})]}{\sinh[\frac{2}{3}(r_0^{3/2} - r_-^{3/2})]}, \quad |x| < l \quad (\text{VM2}). \quad (4.11b)$$

$$J_1 \cong -\gamma_g s_1'^2(x=l) = -\gamma_g s_M^2 \left[ \frac{V}{4bl} \right] \sqrt{r_0 r_+} \operatorname{csch}^2[\frac{2}{3}(r_0^{3/2} - r_+^{3/2})] \quad (\text{VM2}), \quad (4.12a)$$

$$J_2 \cong \gamma_g s_2'^2(x=-l) = \gamma_g s_M^2 \left[ \frac{V}{4bl} \right] \sqrt{r_0 r_-} \operatorname{csch}^2[\frac{2}{3}(r_0^{3/2} - r_-^{3/2})] \quad (\text{VM2}). \quad (4.12b)$$

Using the Simmons approximations, the total current is

$$J = J_1 + J_2 = -4\gamma_g s_M^2 \frac{(\varphi_{MB}^e)^{1/2}}{2b} \left\{ (\varphi_{MB}^e - V)^{1/2} \exp \left[ \frac{-4l}{\sqrt{2b}} \left[ \varphi_{MB}^e - \frac{V}{2} \right]^{1/2} \right] - (\varphi_{MB}^e + V)^{1/2} \exp \left[ \frac{-4l}{\sqrt{2b}} \left[ \varphi_{MB}^e + \frac{V}{2} \right]^{1/2} \right] \right\} \quad (\text{VM2}). \quad (4.13)$$

The comparable expression from quantum mechanics obtained by Simmons<sup>22</sup> for the normal tunneling regime ( $V < \varphi_{MB}^e$ ) is

$$J = \frac{-q^2}{\hbar(4l\pi)^2} \left\{ \left[ \varphi_{MB}^e - \frac{V}{2} \right] \exp \left[ \frac{-4l}{\hbar} (2m^*q)^{1/2} \left[ \varphi_{MB}^e - \frac{V}{2} \right]^{1/2} \right] - \left[ \varphi_{MB}^e + \frac{V}{2} \right] \exp \left[ \frac{-4l}{\hbar} (2m^*q)^{1/2} \left[ \varphi_{MB}^e + \frac{V}{2} \right]^{1/2} \right] \right\}, \quad (4.14)$$

where  $m^*$  is the electron effective mass in the barrier. Equation (4.14) is known to give good agreement with experimental  $I$ - $V$  characteristics for MIM barriers.

Now, in order to make detailed comparisons between the expressions (4.10), (4.13), and (4.14) for the total current, the various macroscopic coefficients in (4.10) and (4.13) must be expressed in terms of microscopic quantities. As noted earlier, for the density-gradient coefficient  $b$  we have the microscopic formula  $b = \hbar^2 / (4rm^*q)$ , where  $r=1$  in the low-temperature, low-density limit<sup>8</sup> and  $r=3$  in the "high"-temperature limit.<sup>9</sup> (In the general case, at least to some extent, the density-gradient theory can be used in a phenomenological fashion with intermediate values of  $r$ .<sup>24</sup>) Employing this formula, we find the exponents in (4.10) and (4.13) to be identical to those of (4.14) if  $r=1$ . That agreement is obtained in the limit of low temperature and low density is consistent with the facts that (4.14) does not include thermionic field emission and that diffusive effects have been neglected in (4.10) and (4.13). This agreement is also not surprising in

that, when  $r=1$  and scattering is negligible, the differential equations of GDD theory are identical to the amplitude part of the Madelung approach to quantum mechanics.<sup>8,13-15</sup> In any event, because of this agreement and because the exponents largely determine the  $I$ - $V$  behavior, we reach the important conclusion that (4.10) and (4.13) will agree just as well with experiment as (4.14). In addition, this comparison suggests that there are regimes, e.g., thermionic field emission, for which effects of  $r$  not being equal to 1 must be considered.

Unfortunately, a similar comparison of the multiplicative coefficients in (4.10), (4.13), and (4.14) cannot be made because we lack microscopic formulas for  $\bar{\gamma}$  and  $\gamma_g$ . Moreover, since the dependences of  $I$ - $V$  data on  $V$ ,  $l$ ,  $T$ , and  $\varphi_{MB}^e$  are largely set by the exponents, such data cannot be used to examine differences between multiplicative coefficients or to assess which downstream boundary conditions are best. For purposes of discussion, we proceed simply by equating the coefficients in (4.10) and (4.13) with those of (4.14) to obtain

$$\frac{e^2}{\hbar(4l\pi)^2} \left[ \varphi_{MB}^e \pm \frac{V}{2} \right] = \frac{4\bar{\gamma}s_M^2(\varphi_{MB}^e)^{1/2}}{(\varphi_{MB}^e \pm V)^{1/2}} \quad (\text{VM1}), \quad (4.15a)$$

$$\frac{e^2}{\hbar(4l\pi)^2} \left[ \varphi_{MB}^e \pm \frac{V}{2} \right] = \frac{4\gamma_g s_M^2}{2b} [\varphi_{MB}^e(\varphi_{MB}^e \pm V)]^{1/2} \cong \frac{4\gamma_g s_M^2}{2b} \left[ \varphi_{MB}^e \pm \frac{V}{2} \right] \quad (\text{VM2}), \quad (4.15b)$$

respectively, where the second equality in (4.15b) assumes  $V \ll \varphi_{MB}^e$ . By this comparison, (4.13) obtained using conditions VM2 corresponds more closely to the result of Simmons, (4.14), since at low voltages the explicit dependences of the multiplicative coefficients on barrier height and voltage are the same

In Fig. 2, we plot the  $I$ - $V$  characteristics for an MIM barrier computed using (4.10), (4.13), and (4.14). The barrier height is 1.5 eV and the barrier thickness is 1.75 nm. For comparison, experimental data from Ref. 25 is shown as well as a numerical solution to (4.2), i.e., with inertia included in the differential equation and using conditions VA. All of the calculations were adjusted to fit the experimental data at low voltages. We note that, although this

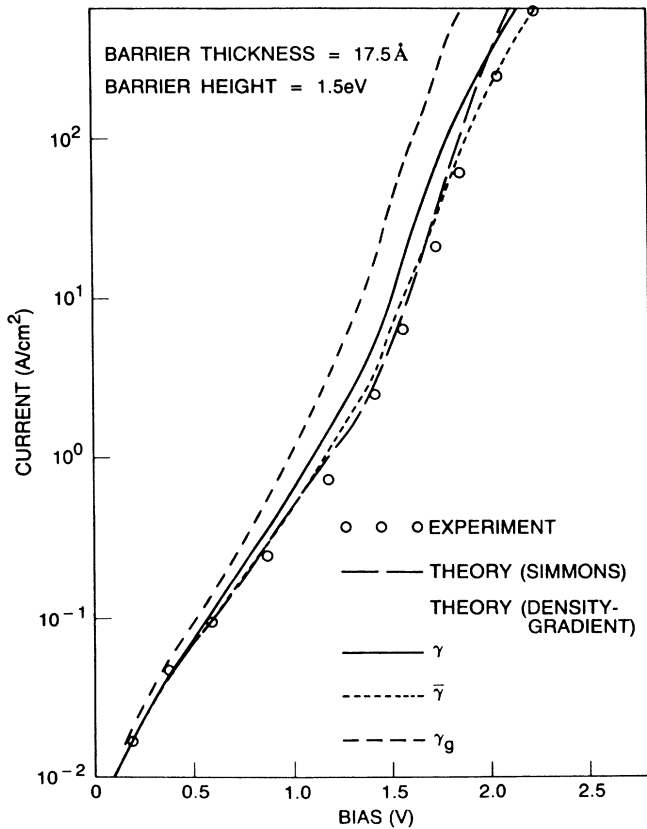


FIG. 2. Comparison of  $I$ - $V$  characteristics for a MIM barrier, 1.5 eV in height and 1.75 nm thick, as measured experimentally in Ref. 25, as computed numerically, and as found using (4.10), (4.13), and (4.14) from Ref. 22. All the calculations were adjusted to fit the experimental data at low voltages and all are in reasonable agreement over the entire voltage range including the Fowler-Nordheim regime.

is standard procedure, the usual fitting parameter is the “active” area which often turns out to be very much smaller than the actual area, e.g., see Ref. 25. In our analysis, instead, only the product of area and  $\gamma$  (or  $\bar{\gamma}$  or  $\gamma_g$ ) is determined by this fitting. And since, at present, the latter is unknown, active areas determined in this way must be regarded as questionable. In any event, when the calculations are fit to data at low voltages we find that all give good agreement with the data over the voltage range  $0 < V < \varphi_{MB}^e$  as well as for the regime with  $V > \varphi_{MB}^e$  which we now discuss.

### B. Regime with $V > \varphi_{MB}^e$ (Fowler-Nordheim)

As we have seen, when  $V < \varphi_{MB}^e$ , both electron gases are governed throughout almost the entire thickness of the barrier by a quasistatic balance between quantum diffusion and electrostatic drift. The change which occurs when  $V$  increases above  $\varphi_{MB}^e$  is that the width of the region over which this balance is maintained can become significantly *less* than the barrier thickness, a situation which may be described as the formation of a quantum boundary layer. Within this layer, the electron charge density decays from its prescribed value of  $s_M^2$  at the upstream contact to a “point,” the boundary layer edge, beyond which  $s$  is small enough that inertia dominates quantum diffusion and the transport becomes ballistic. This boundary layer structure has the nature of a singular perturbation problem.<sup>26</sup> It arises because the highest order derivatives in (4.2) are multiplied by a small parameter (the coefficient  $2b$ ). In the quantum boundary layer (or “inner” region),  $s$  ( $s_1$  or  $s_2$ ) is large,  $\alpha J^2/2s^4$  is negligible and, as earlier, the behavior is quasistatic. Beyond this boundary layer (in the “outer” region),  $s$  has declined sufficiently far that  $\alpha J^2/2s^4$  dominates  $2b(s''/s)$ , the solution is no longer quasistatic and the transport is essentially ballistic. This qualitative understanding of the nature of the solutions to (4.2) leads one to hope that a quantitative analysis based on the methods of singular perturbation theory might be effected. Unfortunately, we have been unable to produce such an analysis and instead resort to other methods. The simplest of these proceeds by application of “virtual-anode” conditions *at the boundary layer edge*. A second approach we examined but will not discuss, involved a singular perturbation type approach with an “intermediate” region solution and a “patching” procedure (rather than the usual matching technique). Lastly, we exhibit full numerical solutions.

The location of the boundary layer edges for  $s_1$  and  $s_2$  can be ascertained by considering (4.3a) and (4.3b). As noted previously, a requirement for quasistatic behavior is that the right sides of these equations be positive. This

means that the profile for  $s_1$  cannot be quasistatic for any  $x$  satisfying  $x_1 < x < l$  and thus the boundary layer edge occurs at  $x = \min(x_1, l)$ . A similar argument applies to  $s_2$ . From the definition of  $x_1$  it is clear that when  $V > \varphi_{MB}^e > 0$ ,  $x_1 < l$ , and quantum boundary layer behavior is obtained. In this case, the region  $-l \leq x \leq x_1$  is the quasistatic inner region (or quantum boundary layer) and  $x_1 \leq x \leq l$  is the outer ballistic transport region. For  $s_2$ , in contrast,  $x_2 < -l$  for all  $V > 0$  and, consequently, the boundary layer always remains thicker than the barrier,  $s_2(x)$  is always quasistatic (except very close to  $x = -l$ ) and all earlier results, including (4.8b) and (4.11b), continue to apply.

As noted above, the “virtual-anode” approach to solving for  $s_1$  when  $V > \varphi_{MB}^e > 0$  employs “boundary” conditions at the boundary layer edge  $x_1$  rather than at  $l$ . As in our earlier analyses, we neglect inertia inside the quantum boundary layer (quasistatic treatment) and subsume its effect entirely in the virtual-anode conditions, i.e., we apply conditions VM1 or VM2 at  $x = x_1$ . When conditions VM1 are used, the solutions for  $s_1$  and  $J_1$  are

$$s_1(x) = s_M \frac{\text{Bi}(r_1) + \sqrt{3}\text{Ai}(r_1)}{\text{Bi}(r_0) + \sqrt{3}\text{Ai}(r_0)}, \quad -l < x < x_1 \quad (\text{VM1}), \quad (4.16a)$$

$$J_1 = \frac{12s_M^2 \hat{\gamma} c_1^2 (\varphi_{MB}^e)^{1/2}}{\pi(2b)^{1/6}} \left[ \frac{2l}{V} \right]^{1/3} \times \exp \left[ \frac{-8l}{3V} \frac{(\varphi_{MB}^e)^{3/2}}{\sqrt{2b}} \right] \quad (\text{VM1}). \quad (4.16b)$$

And when conditions VM2 are used we find

$$J = \frac{e^2}{\hbar(4l\pi)^2} \left\{ \exp \left[ \frac{-4l}{\hbar V} (m^*e)^{1/2} \varphi_{MB}^e{}^{3/2} \right] - \left[ \varphi_{MB}^e + \frac{V}{2} \right] \exp \left[ \frac{-4l}{\hbar} (2m^*e)^{1/2} \left[ \varphi_{MB}^e + \frac{V}{2} \right]^{1/2} \right] \right\}, \quad (4.19)$$

which is known to be in good agreement with many MIM tunneling experiments.

As was the case when  $V < \varphi_{MB}^e$ , when the microscopic connection formula  $b = \hbar^2 / (4rm^*q)$  is used, the exponents in (4.16b) and (4.17b) are identical with that in the first term of (4.19) when  $r=1$ ; that is, in the low-temperature, low-density limit. Again, this means that the predictions of the hydrodynamic theory are in as good agreement with  $I$ - $V$  data as the Simmons expression in the Fowler-Nordheim regime. This agreement was shown in Fig. 2. Finally, as in the normal tunneling regime, comparisons between multiplicative coefficients are not very meaningful because (i) experimental data are only weakly dependent upon them and (ii) we lack microscopic expressions for  $\bar{\gamma}$  and  $\gamma_g$ ; nevertheless, the best functional match is again obtained when conditions VM2 are employed.

The utility of the modified virtual anode conditions VM1 and VM2 as a technique for incorporating inertial effects (quasistatic treatment) and for dealing with quan-

$$s_1(x) = s_M \frac{\text{Bi}(r_1) - \sqrt{3}\text{Ai}(r_1)}{\text{Bi}(r_0) - \sqrt{3}\text{Ai}(r_0)}, \quad -l < x < x_1 \quad (\text{VM2}), \quad (4.17a)$$

$$J_1 = \frac{12s_M^2 \gamma_g c_2^2 (\varphi_{MB}^e)^{1/2}}{\pi(2b)^{5/6}} \left[ \frac{V}{2l} \right]^{1/3} \times \exp \left[ \frac{-8l}{3V} \frac{(\varphi_{MB}^e)^{3/2}}{\sqrt{2b}} \right] \quad (\text{VM2}), \quad (4.17b)$$

where  $c_1 \equiv \text{Ai}(0) \cong 0.355$  and  $c_2 \equiv -\text{Ai}'(0) \cong 0.259$ . In either case, when  $J_1$  is known,  $s_1(x)$  in the outer region ( $x_1 < x < l$ ) can be approximated by the ballistic solution [obtained by neglecting the density-gradient term in (4.2a)] as

$$s_1^2 = J_1 \sqrt{al/V(x-x_1)}, \quad x_1 < x < l. \quad (4.18)$$

We note that (4.18) becomes singular at  $x = x_1$ —indicating that the density-gradient term is non-negligible near  $x = x_1$ —and hence is appropriate only away from this point. This solution may also not be valid near the downstream contact since, as discussed earlier, if the intrinsic “recombination” rate in the contact is finite, “back tunneling” will occur resulting in a quantum boundary layer near  $x = l$ .

The approximate expressions for the total current in the Fowler-Nordheim regime are given by the sum of (4.16b) and (4.9b) when conditions VM1 are used and by the sum of (4.17b) and (4.12b) when conditions VM2 are applied. The corresponding result obtained by Simmons<sup>22</sup> is

tum boundary layer behavior in the Fowler-Nordheim regime is further examined in Figs. 3 and 4. In Fig. 3, as a function of voltage, we plot the values of  $\bar{\gamma}$  and  $\gamma_g$  required for the modified virtual anode approaches to yield the same current as computed numerically from (4.2) assuming  $\gamma$  constant.  $\bar{\gamma}$  and  $\gamma_g$  are seen to vary significantly; however, this variation is only by about a factor of 2 or 3, whereas the current varies by over 7 orders of magnitude in this voltage range, so for computing current these boundary conditions are useful (as was already demonstrated in Fig. 2). We remark that, for unknown reasons, the conditions VM1 do especially well in the Fowler-Nordheim regime with  $\bar{\gamma}$  about a factor of 10 smaller than  $\gamma$ .

Figure 4 compares electron density ( $s_1^2$  only) profiles inside of an MIM barrier as computed analytically using the modified virtual-anode approaches with that found by solving (4.2) numerically. This is, of course, a much more stringent test of the approximations than comparisons between predicted current because here we examine the lo-

cal solution. The barrier for these calculations has the same height and width as was assumed for Figs. 2 and 3 and the applied bias is in the Fowler-Nordheim regime with  $V = 2\varphi_{MB}^e$ . The numerical calculation shows the expected behavior with an exponentially decaying quantum boundary layer and a smooth transition into the classical (ballistic) transport region. In contrast, none of the analytical solutions are particularly good with that based on VM1 doing the best. As expected, the worst agreement is obtained in the vicinity of the transition region where (4.18) breaks down.

The various solutions to the MIM barrier problem developed above exhibit a number of the known features of quantum-mechanical tunneling current. The demonstrated correspondences between the macroscopic equations and microscopically derived results show that the density-gradient hydrodynamic description of Ref. 6 is indeed capable of describing important lowest-order quantum effects in transport situations. Moreover, this field theory description of tunneling resulted from the addition of the same new term in the diffusion-drift current

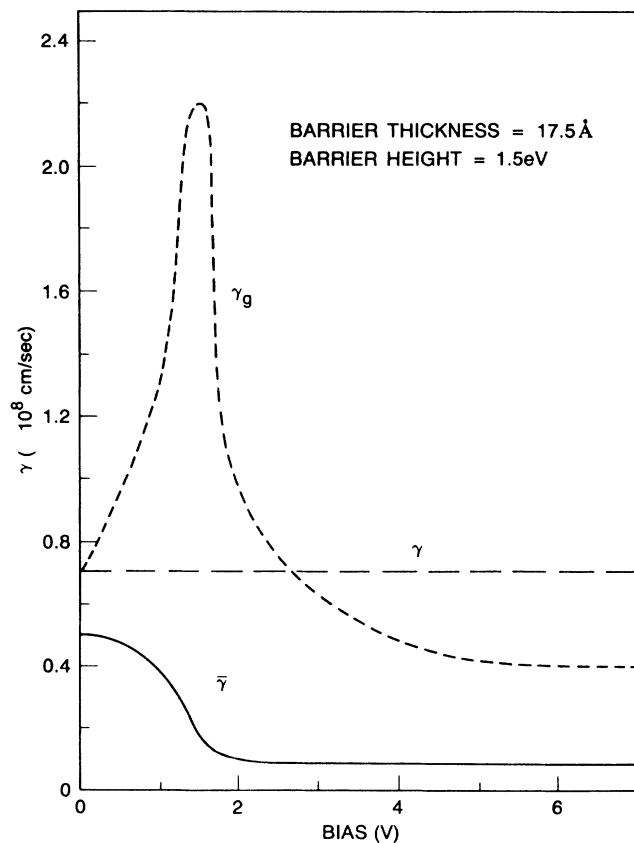


FIG. 3. Values for  $\bar{\gamma}$  and  $\gamma_g$  required to give the same current computed assuming  $\gamma$  constant are plotted as a function of bias for the same barrier as in Fig. 2. While  $\bar{\gamma}$  and  $\gamma_g$  vary significantly, this variation is small compared to the current variation thus demonstrating that treating inertia via downstream boundary conditions is a useful approximation.

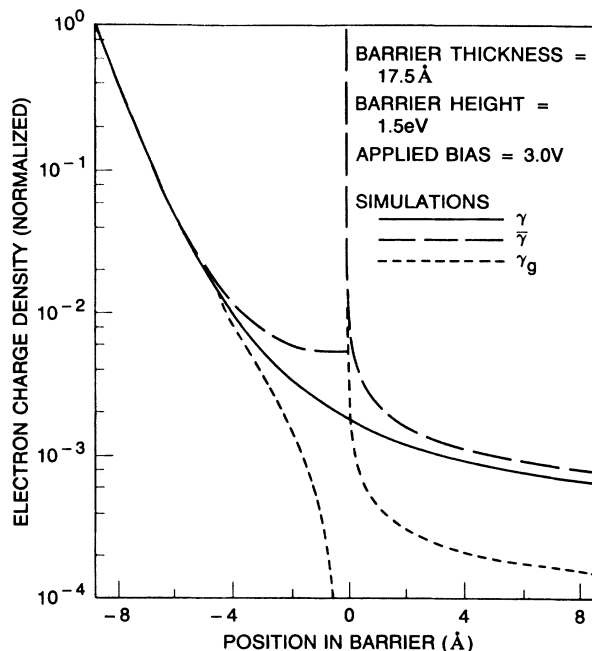


FIG. 4. Comparison between electron-density profiles ( $s_1^2/q$ ) inside the same MIM barrier as Fig. 2 with an applied bias of 3 V as computed numerically and from (4.16a), (4.17a), and (4.18). Except near the boundary layer edge ( $x = x_1 = 0$ ) the analytical formulas are in reasonable agreement with the numerical result.

equation—the “quantum diffusion” term—which previously had permitted description of macroscopic quantum confinement effects.<sup>6–8</sup> Fundamentally, these new capabilities of diffusion-drift theory stem from the fact that the effect of quantum mechanics on electrons in a semiconductor (apart from effects of quantum statistics) is, to lowest order, equivalent to having an electron gas whose equation of state is density-gradient dependent.

#### V. STEADY-STATE MIM TUNNELING: BULK-SCATTERING-DOMINATED CASE

This section briefly discusses a tunneling regime in which drag is significant, inertia is negligible, and the scattering inside the barrier (including electron-electron scattering) is strong enough that a *single* electron gas model is appropriate (see Sec. III). We again emphasize that drag is here treated via the linear drag law (2.5) (or relaxation time approximation<sup>21</sup>) which is of uncertain validity. With these simplifications (and again assuming that space-charge effects and normal diffusion are negligible), the transport equation (2.8) becomes

$$\frac{J}{\mu^e s^2} + \varphi' - 2b \left[ \frac{s''}{s} \right]' = 0. \quad (5.1)$$

The electric potential is again given by (4.1) and the boundary conditions on the electron gas—assuming *both* contacts are ideal with respect to transport—are

$$s = s_M \text{ at } |x| = l, \quad (5.2a)$$

$$\varphi^{e*} = \varphi_M^e \text{ at } |x| = l. \quad (5.2b)$$

An approximate solution to (5.1) with (5.2) can be obtained by first formally integrating to obtain

$$2b \frac{s''}{s} = E_0(x-l) + K_1 - \frac{J}{\mu^e} f(x) \equiv g(x), \quad (5.3a)$$

where

$$f(x) \equiv \int_{-l}^x \frac{dx}{s^2}. \quad (5.3b)$$

The solution  $s$  to (5.3) decays exponentially from its large values at the contacts ( $s_M$ ) to a minimum value at some unknown location  $x_m$  inside the barrier. When zero bias is applied  $x_m = 0$ . Because of the exponential character of the decay, the integrand in (5.3b) is sharply peaked about  $x_m$  and  $f(x)$  will be a steplike sigmoid with the step located at  $x_m$ . Approximating the sigmoid  $f(x)$  as a linear step of unknown height [ $f(l)$ ], slope and location, (5.3) becomes an Airy equation whose solution (using the WKB approximation) is

$$s \cong s_M g^{-1/4} (K_2 e^{p(x)} + K_3 e^{-p(x)}), \quad (5.4)$$

where

$$p(x) \equiv \frac{1}{\sqrt{2b}} \int_{-l}^x \sqrt{g(t)} dt.$$

Then, using (5.2), we find  $f(l)$  to be  $-\mu^e V/J$ ,

$$J = -\mu^e V s_M^2 (\varphi_{MB}^e / 2b)^{1/2} \text{csch}[p(l)], \quad (5.5)$$

and  $p(l)$  and  $x_m$  to be determined by

$$\frac{V}{4g(x_m)} \cong \sinh[2p(x_m) - p(l)] \quad (5.6a)$$

with

$$p(l) \cong \frac{4l}{3V\sqrt{2b}} \left[ \left[ \varphi_{MB}^e - \frac{V}{2}(1+x_m/l) \right]^{3/2} - \left[ \varphi_{MB}^e + \frac{V}{2}(1-x_m/l) \right]^{3/2} \right], \quad (5.6b)$$

$$p(x_m) \cong \frac{4l}{3V\sqrt{2b}} \left[ \left[ \varphi_{MB}^e - \frac{V}{2}(1+x_m/l) \right]^{3/2} - (\varphi_{MB}^e)^{3/2} \right]. \quad (5.6c)$$

To some extent these equations apply also to the Fowler-Nordheim regime, however, the assumption that  $f(x)$  is a linear step becomes increasingly poor. Nonetheless, for this regime the physically important point is that, in a similar way to the inertia-dominated case, a transition occurs from quantum diffusive transport in a quantum boundary layer near  $x = -l$  to classical transport—in this case, pure drift—throughout most of the rest of the structure. Of course, near  $x = l$ , the density must increase to match the condition  $s = s_M$  at  $x = l$  and thus a small quantum boundary layer will also exist at this boundary as well.

A plot of the scattering-dominated tunneling current as a function of the voltage is shown in Fig. 5. For comparison, the numerically calculated  $I$ - $V$  curve for inertia-dominated tunneling is also shown. As with Fig. 2 the multiplicative coefficients have been selected so that the curves agree at low voltages. The characteristics are qualitatively different from each other and the scattering-dominated curve clearly does not correspond to typical experimental results. This lack of agreement cannot be corrected by a simple adjustment of various parameters, e.g.,  $\varphi_{MB}^e$  or  $l$ . Whether any experimental data exists in agreement with this prediction is unclear. Microscopically, plausible criteria for obtaining this regime are that the voltage be low, the elastic mean free path be smaller than the barrier thickness and the inelastic mean free path (coherence length) be larger than the barrier thickness. This is an unusual combination but perhaps an experimental investigation is warranted.

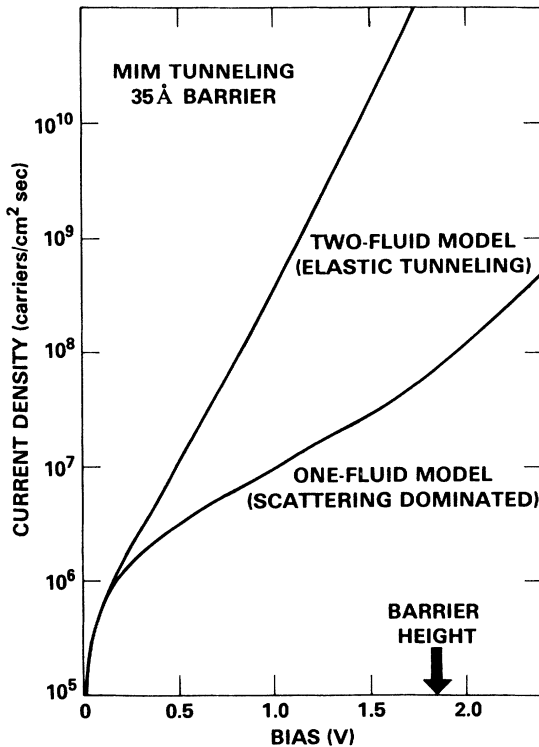


FIG. 5. Comparison between  $I$ - $V$  characteristics computed numerically for an MIM barrier 3.5 nm in thickness and 1.8 eV in height for inertia-dominated tunneling (two-fluid model) and bulk-scattering-dominated tunneling (one-fluid model). The curves are qualitatively different with the former agreeing well with experiment (not shown).

## VI. SUMMARY AND CONCLUSIONS

In this paper, the previously developed macroscopic description of electron transport in semiconductors in which lowest-order quantum effects have been accounted

for through a density-gradient term has been applied to a quantum transport problem. Electron tunneling through an MIM barrier has been analyzed for both inertia-dominated and bulk-scattering-dominated regimes by solving appropriate boundary value problems. With the aid of "virtual-anode" boundary conditions which account for dissipation in the downstream contact, we find that the  $I$ - $V$  characteristics for inertia-dominated tunneling are in good agreement both with tunneling experiments and with calculations from one-electron quantum mechanics. The  $I$ - $V$  characteristics for scattering-dominated tunneling are qualitatively different and it is uncertain whether this regime is ever physically realized.

The ability of the theory to describe single-barrier tunneling using a hydrodynamic description, as demonstrated in this paper, suggests that the density-gradient approach to quantum transport modeling has real potential

for semiconductor device simulation. By including quantum effects to lowest order only, the approach is capable of describing the important phenomena of quantum confinement and quantum tunneling yet, at the same time, the description is simple enough that other complications of real devices such as electrostatics or geometry can be analyzed.

#### ACKNOWLEDGMENTS

The author wishes to thank Professor H. F. Tiersten of Rensselaer Polytechnic Institute for numerous discussions including one many years ago in which the possibility, in principle, of a continuum description of tunneling was recognized. The long-term support of the U.S. Naval Research Laboratory is gratefully acknowledged.

- <sup>1</sup>W. Van Roosbroeck, *Bell Syst. Tech. J.* **29**, 560 (1950).
- <sup>2</sup>K. Blotekjaer, *IEEE Trans. Electron Dev.* **ED-17**, 38 (1970).
- <sup>3</sup>K. K. Thornber, *IEEE Electron Dev. Lett.* **EDL-3**, 69 (1982).
- <sup>4</sup>L. Reggiani, in *Hot-Electron Transport in Semiconductors*, edited by L. Reggiani (Springer-Verlag, Berlin, 1985), Chap. 2.
- <sup>5</sup>W. Frensley, *Phys. Rev. B* **36**, 1570 (1987).
- <sup>6</sup>M. G. Ancona and H. F. Tiersten, *Phys. Rev. B* **35**, 7959 (1987). The detailed derivations of this paper plus the changes necessary when inertia is important appear in NRL Memorandum Report NO. 6444, 1989, available upon request.
- <sup>7</sup>M. G. Ancona, *COMPEL-Int. J. Comp. Math. Elect. Eng.* **6**, 11 (1987).
- <sup>8</sup>M. G. Ancona, *Superlatt. Microstruct.* (to be published).
- <sup>9</sup>M. G. Ancona and G. J. Iafrate, *Phys. Rev. B* **39**, 9536 (1989).
- <sup>10</sup>Partial results from this work appeared in *Bull. Am. Phys. Soc.* **33**, 786 (1988), and in Proceedings of the 1st International Vacuum Microelectric Conference, Williamsburg, Virginia, 1988 (unpublished).
- <sup>11</sup>A higher-order quantum-mechanical effect not captured by the density-gradient theory is the quantum reflection phenomenon observed in some tunneling experiments; e.g., see J. Maserjian, *J. Vac. Sci. Technol.* **11**, 996 (1974).
- <sup>12</sup>The notion of a planar-averaged continuum theory (Ref. 6) plus the fact that the changes themselves are spread out by the Pauli principle lead one to expect that the continuum approach will be particularly robust.
- <sup>13</sup>E. Madelung, *Z. Phys.* **40**, 332 (1926).
- <sup>14</sup>L. de Broglie, *Non-linear Wave Mechanics* (Elsevier, Amsterdam, 1960).
- <sup>15</sup>D. Bohm, *Phys. Rev.* **85**, 166 (1952).
- <sup>16</sup>J. V. Lill, M. I. Haftel, and G. H. Herling, *J. Chem. Phys.* **90**, 4940 (1989).
- <sup>17</sup>H. Grad, *Commun. Pure Appl. Math.* **2**, 331 (1949).
- <sup>18</sup>D. Burnett, *Proc. London Math. Soc. (Ser. 2)* **40**, 382 (1936).
- <sup>19</sup>C. B. Duke, *Tunneling in Solids in Solid-State Physics*, Suppl. 10 (Academic, New York, 1969).
- <sup>20</sup>M. G. Ancona and H. F. Tiersten, *Phys. Rev. B* **22**, 6104 (1980).
- <sup>21</sup>This approach is equivalent to the use of a simple relaxation-time approximation in the Wigner-Boltzmann equation, e.g., see Refs. 5 and 9.
- <sup>22</sup>J. G. Simmons, *J. Appl. Phys.* **34**, 1793 (1963).
- <sup>23</sup>The words "surface recombination condition" and "surface recombination velocity" refer, of course, to the similarity between (3.5b) and the well-known Shockley surface recombination boundary condition [W. Shockley, *Bell Syst. Tech. J.* **28**, 435 (1949)]. In addition to having the same form, we note that neither (3.5b) nor the Shockley condition is applied at an actual physical boundary and that, for both, the recombination velocity is not simply a material surface coefficient but depends on bulk properties also.
- <sup>24</sup>This statement is based entirely on numerical calculations for equilibrium situations (Ref. 8); we have no general proof.
- <sup>25</sup>S. R. Pollack and C. E. Morris, *Trans. Metall. Soc. AIME* **233**, 497 (1965).
- <sup>26</sup>The singular nature of (3.1c) associated with the small parameter multiplying  $d^2\varphi/dx^2$  is well known to semiconductor device modelers, e.g., see P. A. Markowitch, *The Stationary Semiconductor Device Equations* (Springer-Verlag, New York, 1986), Chap. 4. The singular nature of (3.1a) and (3.1b), arising from the small parameter multiplying  $d/dx [(1/s)(d^2s/dx^2)]$ , shares the same physical origin (small size of  $b$  or  $h$ ) as the singular behavior of the Schrödinger equation. It is of interest to note, however, that mathematically the singular behavior of (3.1a) and (3.1b) and of the Schrödinger equation differ in character. The latter equation often exhibits wavelike solutions which break down globally as the small parameter vanishes. In contrast, for (3.1a) and (3.2b) solutions always decay and the breakdown is localized in boundary layers.